

# Epoxy/Alumina Nanoparticle Composites. I. Dynamic Mechanical Behavior

E. Vassileva, K. Friedrich

*Institute for Composite Materials (IVW), University of Kaiserslautern, D-67663 Kaiserslautern, Germany*

Received 13 June 2002; accepted 25 November 2002

**ABSTRACT:** We studied the influence that alumina nanoparticle addition has on the dynamic mechanical spectra of an amino-cured epoxy resin. A suppression of the short-scale cooperative motions related to the  $\beta$  relaxation and an increase in the activation energy for the  $\beta$  relaxation of the epoxy matrix was observed as the alumina content increased. This is explained in terms of an antiplasticization effect of the alumina nanoparticles on the epoxy resin. An estimation of the effective thickness of the nanoparticle–matrix interfacial region was done based on the reduced damping. The dependence of the composites' reduced mod-

ulus on the alumina nanoparticles content is very well fitted by the generalized Kerner equation. The best-fit parameter values suggest the presence of small and strong agglomerates in the composites at room temperature. At temperatures above the  $T_g$ , these agglomerates start to behave as weak ones because of the polymer matrix softening and particle–particle and particle–matrix slippage and friction. © 2003 Wiley Periodicals, Inc. *J Appl Polym Sci* 89: 3774–3785, 2003

**Key words:** nanoparticles; viscoelastic properties; activation energy

## INTRODUCTION

It is well known that an amino-cured epoxy resin has three relaxation processes in its dynamic mechanical spectra, that is, two at low temperature,  $\gamma$  and  $\beta$  relaxation, and one at high temperature,  $\alpha$  relaxation. The  $\gamma$  relaxation (approximately  $-150^\circ\text{C}$ ) is due to motions of the flexible central parts of sufficiently long aliphatic sequences. These sequences could be contained either in the epoxy or in the amine moieties, so the  $\gamma$  relaxation does not always appear. The  $\beta$  relaxation (approximately  $-60^\circ\text{C}$ ) is a result of the motions of the hydroxypropylether units together with the flips of the benzene rings of diglycidyl ether of bisphenol A.<sup>1,2</sup> It occurs whatever the chemical nature of the hardener is. The  $\alpha$  relaxation is interpreted as the onset of long-range, coordinated molecular motions.

Recently, it was shown by dynamic mechanical thermal analysis (DMTA) and NMR experiments that in a dense amino-cured epoxy network the  $\beta$  relaxation can be separated in a low- and a high-temperature part.<sup>1,2</sup> The low-temperature part is due to local motions at the spatial scale of one epoxy–amine repeat unit. Cooperative motions involving at least six units are responsible for the high-temperature part of the  $\beta$  relaxation.<sup>1</sup> While the local motions are not affected at

all, the short-scale cooperative motions are strongly influenced by an antiplasticizer incorporation.<sup>2</sup>

In general, a diluent is said to plasticize a polymer when the polymer modulus decreases with the diluent addition. This is associated with an increase of the mechanical loss below the glass transition. When the diluent increases the polymer modulus, it is designed as an antiplasticizer and then the mechanical loss is lower.<sup>3</sup> A diluent can act as an antiplasticizer when it is added to the polymer at low concentration and as a plasticizer when its content is higher. The antiplasticizer increases the apparent activation energy of the secondary relaxation as well as its spread. As a consequence, the number of the motion units contributing to the secondary relaxation decreases and, respectively, the strength of the relaxation decreases.<sup>4</sup> A good description of the antiplasticization–plasticization phenomena in a polymer glass gives the lattice model.<sup>3</sup> According to this model, the first diluent molecule, which comes into contact with a polymer repeat unit, is assumed to reduce the mobility of the unit and to improve the local packing, which results in densification of the polymer. It acts in this way as long as it is an isolated diluent molecule. This is the regime of simple antiplasticization according to the lattice model. As the diluent concentration increases, the diluent molecules start to form clusters. The polymer repeat units already do not contact with an isolated diluent molecule but with clusters from diluent molecules, which results in an increased mobility of the polymer chains and, hence, the plasticization effect of the diluent starts.

Correspondence to: K. Friedrich (friedrich@ivw.uni-kl.de).

Contract grant sponsor: European Community; contract grant number: HPMF-CT-2000-00864.

Ngai et al.<sup>4</sup> applied the coupling model of relaxation for explaining the antiplasticization of the  $\beta$  relaxation in polycarbonates of bisphenol A. The coupling model describes the effects which the intermolecular coupling has on the relaxation rate of an intramolecular motion. When the polymer chain has sufficiently localized intramolecular motions, it is expected to have an uncoupled relaxation rate which is unaffected by the intermolecular coupling. The local free volume and the energy barrier that should be surmounted in executing the relaxation motion determine the uncoupled relaxation rate. When intermolecular coupling takes place, the coupling model asserts that the uncoupled relaxation rate is reduced by a time-dependent factor of the form  $t^{-n}$ . Here,  $t$  is the time and  $n$  is a coupling parameter, introduced to count for the strength of the intermolecular coupling. A zero value of the coupling parameter means that the relaxation does not couple to other molecules. In the framework of the coupling model, the antiplasticization of the secondary relaxation in polycarbonates of bisphenol A follows as a consequence of the increase in its coupling parameter  $n$  when a diluent is added.

The plasticizers in polycarbonates of bisphenol A, according to Ngai et al.,<sup>4</sup> hinder the benzene ring mobility, while, on the other hand, they facilitate the segmental mobility. They drastically broaden the relaxation spectrum of the phenyl ring motion but leave that of the segmental motion ( $\alpha$  relaxation) unchanged or possibly even narrow it. These opposite effects that the plasticizers have on the secondary and primary (segmental) relaxations justify, according to the authors,<sup>4</sup> the use of the term "antiplasticization" to describe the effects that they have on the secondary relaxation. Originally, the term antiplasticization was used to describe the property of a plasticized polymer in the glassy state at temperatures well below the  $T_g$  to be harder and more brittle than is the neat polymer.<sup>2</sup>

Not all diluents have an antiplasticization effect and Ngai et al.<sup>4</sup> explained this fact with the  $T_g$  values for the pure diluent. If the secondary relaxation of the polymer appears at temperatures well above the  $T_g$  of the diluent, the molecules of the diluent relax very fast compared to the polymer macromolecules. Thus, the polymer relaxation motions will be not constrained because of the diluent molecules' presence and, hence, the diluent will act as a typical plasticizer. In this case, the diluent is close to its own  $T_g$  at the temperature of the polymer secondary relaxation; its molecules could have relaxation times comparable with those for the polymer, so the constraints on the relaxation motions will be enhanced and the antiplasticization effect will appear.

Heux et al.<sup>2</sup> investigated in detail the antiplasticization of an amine-cured epoxy resin. They pointed out that

- The antiplasticizer has no effect on the local molecular motions in the epoxy resin (i.e., on the low-temperature part of the  $\beta$  relaxation).
- The antiplasticizer hinders all motions with a short-range cooperative character, contributing to the high-temperature part of the  $\beta$  relaxation.

The dependence of the modulus, the strength, and the elongation at break on the diluent content for an antiplasticized polymer seems very similar to the dependence of the same properties on the filler content for nanoparticle-filled composites. We assumed that if the filler particles are small enough (of nanosize) and if they are well dispersed in the polymer matrix (at the nanolevel), they should behave as an antiplasticizer, suppressing the short-scale cooperative motions in the polymer matrix. Thus, the activation energy for the sub- $T_g$  relaxations should be increased, as is the case for an antiplasticized polymer glass. To check the validity of this assumption, we studied in detail the dynamic mechanical properties of an amino-cured epoxy resin filled with alumina nanoparticles.

A very helpful tool in studying the cooperativity and/or the local character of viscoelastic relaxations is the Starkweather analysis.<sup>5</sup> It has been applied successfully for neat and antiplasticized amine-cured epoxy resins.<sup>1,2</sup> The relaxations, according to the Starkweather analysis, could be classified into simple (non-cooperative) and complex (cooperative) ones, according to the value of their activation entropy. The simple relaxations have zero or small positive or negative values for their activation entropy. The activation entropy could deviate from the zero value within experimental uncertainty, which is at least  $\pm 4.17$  kJ/mol.<sup>5</sup> These relaxations involve the motions of small groups of atoms, which interact very little with other parts of the same or of neighboring molecules. Samples for simple relaxations are the motions of the side groups attached to the main chain. Also, most of the relaxations due to the alkyl groups at the end of the side groups and relaxations associated with dissolved small molecules have a zero activation entropy.

When the relaxations have large activation entropies, they are designated as complex. The complex relaxations involve a spectrum of related motions with extensive intra- and intermolecular motions.<sup>5</sup> They are usually related to main-chain motions.

The activation enthalpy and entropy for one relaxation are estimated on the basis of its activation energy. The activation energy could be determined from the frequency-temperature dependence of the relaxation expressed in terms of the Arrhenius equation:

$$f = Ae^{-E_{\text{act}}/RT} \quad (1)$$

Here,  $f$  is the frequency in Hz;  $A$ , a preexponential constant;  $R$ , the gas constant;  $T$ , the absolute temper-

ature in K; and  $E_{\text{act}}$ , the activation energy of the relaxation. The activation enthalpy  $\Delta H^\ddagger$  and entropy  $\Delta S^\ddagger$  of the relaxation are related to its activation energy as follows<sup>5</sup>:

$$\Delta H^\ddagger = E_{\text{act}} - RT' \quad (2)$$

and

$$\Delta S^\ddagger = \{E_{\text{act}} - RT'[1 + \ln(kT'/2\pi h)]\}/T' \quad (3)$$

Here,  $T'$  is the maximum temperature of the relaxation peak, observed at 1 Hz, and  $R$ ,  $k$ , and  $h$  are, respectively, the gas, Boltzman's, and Plank's constants. When the activation entropy is zero ( $\Delta S^\ddagger = 0$ ), eq. (3) could be written as follows:

$$E_{\text{act}} = RT'[1 + \ln(kT'/2\pi h)] \quad (4)$$

The simple, or noncooperative, relaxations have activation energy, which is on or very close to the zero activation entropy line, drawn according to eq. (4). The activation energy of the complex relaxations is far away from the zero activation entropy line.

The dynamic mechanical behavior of particulate-filled composites has been well studied over recent years. Some common effects of rigid fillers on the dynamic mechanical properties of composites are<sup>6</sup>

1. Increasing of the modulus to a higher extent above the  $T_g$  than below it.
2. Broadening of the damping peak accompanied by a slight shift to higher temperatures.
3. Fillers often decreasing the damping, which can generally be approximated by

$$\tan \delta_c = \tan \delta_m V_m + \tan \delta_f V_f \quad (5a)$$

Here,  $V_f$  and  $V_m$  refer to the volume fractions of the filler and matrix, respectively, whereas  $\tan \delta_c$  and  $\tan \delta_m$  represent the loss tangent values of the composite and the neat matrix, respectively. The damping of most rigid fillers is very low compared to the damping of the polymers, so that the second term in eq. (5a) could be neglected:

$$\frac{\tan \delta_c}{\tan \delta_m} = V_m = (1 - V_f) \quad (5b)$$

Sometimes, fillers can also increase the damping of composites, and this is usually, but not always, related to an introduction of new damping mechanisms. Possible new damping mechanisms are (1) particle-particle slippage or friction when the particles touch each other as in weak agglomerates, (2) particle-polymer friction when there is no adhesion at the filler-matrix

interface, and (3) increasing of the damping in the polymer near the filler-matrix interface because of thermal stresses or being induced by the filler changes in the polymer conformation and morphology.<sup>7</sup>

When a significant interaction exists between the matrix and the filler, a layer of polymer surrounding each filler particle is formed. Thus, an immobilized polymer layer is created around the filler particles, which indirectly increases the effective filler volume fraction in the composite and causes a mechanical coupling effect between the matrix and the filler. As a result of such a polymer-filler interaction, eq. (5b) is rewritten with the introduction of a correction parameter  $P$  (ref. 8):

$$\tan \delta_c = \tan \delta_m (1 - PV_f) \quad (6)$$

The correction parameter  $P$  is related to the effective thickness of the particle-matrix interfacial region  $\Delta R$  through<sup>8</sup>

$$P = (1 + \Delta R/R)^3 \quad (7)$$

Here,  $R$  is the radius of the dispersed particles.

One of the best models describing the modulus dependence on the filler content for polymer composites is the generalized Kerner equation<sup>6,7</sup>:

$$\frac{M_{\text{composite}}}{M_{\text{matrix}}} = \frac{1 + ABV_f}{1 - B\Psi V_f} \quad (8)$$

Here,  $M$  is any modulus (shear, Young's, bulk);  $A$ , a constant dependent on the geometry of the filler phase and the Poisson's ratio of the matrix; and  $B$ , a constant related to the ratio  $M_{\text{filler}}/M_{\text{matrix}}$ . For very large  $M_{\text{filler}}/M_{\text{matrix}}$  ratios,  $B$  is 1:

$$B = \frac{(M_{\text{filler}}/M_{\text{matrix}}) - 1}{(M_{\text{filler}}/M_{\text{matrix}}) + A} \quad (9)$$

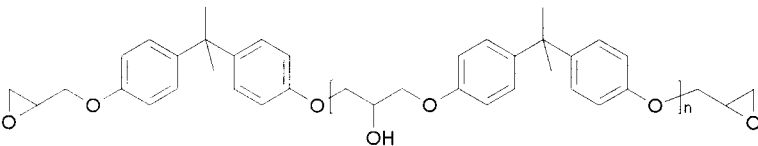
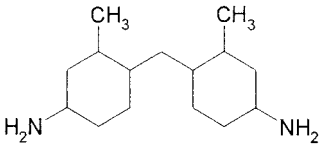
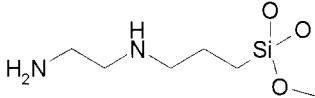
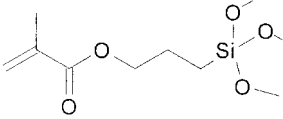
$\Psi$  is a reduced concentration term, which depends on the maximum packing fraction  $\Phi$  of the particles. Nielsen<sup>6</sup> defined the reduced concentration term  $\Psi$  as

$$\Psi = 1 + \frac{1 - \Phi_m}{\Phi_m^2} V_f \quad (10)$$

McGee et al.<sup>6</sup> proposed a different equation for  $\Psi$  when the filler modulus is much higher than is the matrix modulus and when agglomeration exists in the system:

$$\Psi = 1 + \frac{V_m}{\Phi_m} [\Phi_m V_f + (1 - \Phi_m) V_m] \quad (11)$$

TABLE I  
Chemical Structures of the Epoxy Resin, Hardener, and SCAs, Used in This Work

Substance	Chemical structure
Epoxy resin DER 331	
2,2'-Dimethyl-4,4'-methylenebis(cyclohexylamin)	
-[3-(2-Aminoethylamino)propyl]-trimethoxysilane (RSCA)	
3-(Trimethoxysilyl)propyl methacrylate (NRSCA)	

The maximum packing fraction  $\Phi_m$  has a maximum theoretical value of 0.74 for spheres in the case of a hexagonal close packing. This parameter varies with the particles' shape and state of agglomeration. Agglomerates and nonspherical particles generally have smaller  $\Phi_m$  values than those of spheres.<sup>6</sup>

The constant  $A$  in the case of spherical filler particles and for any Poisson's ratio  $\nu$  of the matrix is defined as

$$A = \frac{7 - 5\nu}{8 - 10\nu} \quad (12)$$

If the particles are not well dispersed and form agglomerates, the constant  $A$  increases. In this study, we applied the modified Kerner equation for the epoxy/alumina nanoparticle composites to describe their reduced modulus dependence on the alumina nanoparticle content. Also, we tried to estimate the alumina nanoparticle-epoxy matrix interaction using the reduced damping dependence on the alumina nanoparticles content.

## EXPERIMENTAL

### Materials

General-purpose epoxy resin DER 331, reaction product of epichlorhydrin and bisphenol-A (Dow Chemical, Ibbenbueren, Germany), was used as a matrix. The hardener, 2,2'-dimethyl-4,4'-methylenebis(cyclohexylamin), was purchased from Vantico Ltd. (Bergkamen, Germany). Alumina nanoparticles,  $\text{Al}_2\text{O}_3$ , with a size of 40 nm and a specific surface area of 41  $\text{m}^2/\text{g}$ , were

purchased from Nanophase Technologies Corp. (Romeoville, IL)

Two silane coupling agents (SCAs) were used for nanoparticle treatment, namely, [3-(2-aminoethylamino)propyl]trimethoxysilane (RSCA) and 3-(trimethoxysilyl)propyl methacrylate (NRSCA), purchased from Gelest Inc. (Karlsruhe, Germany). Their chemical structures together with the structures of the epoxy resin and the hardener are shown in Table I. The first SCA can react via its amino groups with the epoxy groups of the matrix, and it is designated as a reactive silane coupling agent (RSCA). The second one cannot react chemically with the matrix, and it is designated as a nonreactive silane coupling agent (NRSCA).

### Nanoparticles treatment with SCAs

The amount of SCAs (in grams) ( $ASCA$ ) necessary to obtain a minimum multilayer coverage onto the particles is calculated using the specific wetting surface ( $sws$ ) of the SCA:

$$ASCA = \frac{AF \times saf}{sws} \quad (13)$$

Here,  $saf$  is the surface area of the filler in  $\text{m}^2/\text{g}$  and  $AF$  is the amount of the filler in grams.

### Composites preparation

The resin and the nanoparticles are mixed together in a special dispersing device. Nanoparticles, if non-



treated, are dried preliminary for 12 h at 70°C. The mixture is evacuated at 60°C to remove any traces of air or to evaporate the solvent when treated nanoparticles are used. Then, the mixture is cooled to 27°C, and the dispersion is performed for 30 min at a speed of 5800 rpm. The hardener is added in an amount of 1/3 of the resin weight. The final mixture is poured into aluminum forms and put into an oven where curing is performed at first for 8 h at 70°C and then for another 16 h at 120°C. The nanoparticle volume content used in this study was in the range of 1–15 vol %, which, in terms of weight %, means from 3 to 37 wt %.

### Composites' characterization

Differential scanning calorimetry (DSC) was performed using a Mettler Toledo DSC 821e in the temperature range between 30 and 270°C (at a heating rate of 10°/min), using a heating/cooling/heating mode. The apparatus was calibrated using indium. The  $T_g$  values were evaluated from the middle point of the transition. In the same heating/cooling/heating mode, a DSC scan for an empty aluminum pan was done. Before the  $T_g$  evaluation, from each DSC scan, the DSC signal obtained for the empty aluminum pan in the same mode was subtracted (blanc correction).

DMTA was performed using a GABO Qualimeter Eplexor 150 N. All samples were tested in the three-point bending mode, using a sample size of  $32 \times 10 \times 3$  mm. The temperature range varied from  $-150$  to  $270^\circ\text{C}$ , applying heating steps of  $2^\circ/\text{min}$ . The temperature dependence of the loss modulus  $E''$  served for the determination of the transition temperatures and the activation energies.

From the storage modulus values at  $T_g + 50$ ,  $E'_{T_g+50}$ , (in the rubbery plateau region), the network density was determined using the following relationship<sup>9</sup>:

$$E'_{T_g+50^\circ\text{C}} = 3qnRT = 3q(d/M_c)RT \quad (14)$$

Here,  $q$  is the front factor, usually equal to 1;  $n$ , the apparent crosslinking density;  $R$ , the gas constant ( $R = 8.314 \text{ J/Kmol}$ );  $d$ , the density of the material; and  $T$ , the absolute temperature in K. Originally, this formula was utilized for a homogeneous single phase, but it also gives very good results for two-phase rubber-toughened epoxy resin systems.<sup>9</sup> The values obtained by this equation are used only for comparing the network density of the samples investigated in this work.

## RESULTS AND DISCUSSION

### Results from the DSC experiment

The DSC curves obtained in the second heating scan for all epoxy/alumina nanoparticle composites to-

gether with the neat epoxy matrix are presented in Figure 1(a). All these curves are blanc corrected, i.e., from the corresponding originally obtained DSC curves, the curve obtained with an empty alumina pan is subtracted. The values of the glass transition temperatures detected in the first and the second heating scans of the DSC experiment are presented in Table II. Their alumina content dependence is more clearly presented in Figure 1(b), where it is easily seen that  $T_g$  increases as the alumina content increases and levels off for a higher alumina content. A similar increase of  $T_g$  with an increasing filler content was reported for a large number of particulate-filled composites. Usually, it is considered to be due to the filler–matrix interaction.<sup>8</sup> But as Lee and Nielson<sup>10</sup> showed, the increase in  $T_g$  could be also due to an increase in the filler particle agglomeration. For the present system of epoxy/alumina nanoparticle composites, the increase of  $T_g$  (decrease in the segmental mobility) with increase of the alumina content could be explained by each of the following reasons: (1) increased filler–matrix interaction and (2) increased alumina nanoparticle agglomeration.

The values of  $T_g$ , obtained in the first heating DSC scan, are higher than the values obtained in the second one [Fig. 1(b)]. Two processes could be responsible for this behavior, both taking place during the DSC experiment: (1) drying and/or (2) an additional curing of the epoxy resin.

The glass transition temperatures for both epoxy/SCA-treated alumina nanoparticle composites are also shown in Table II. In the first heating scan, both samples have almost the same  $T_g$ , which is lower than the  $T_g$  of the sample containing the same amount (3 vol %) of nontreated alumina nanoparticles [Fig. 1(b)]. This lower  $T_g$  could be explained by the plasticizing effect of the nonreacted part of SCA and/or by the increased water absorption of the samples because of the SCA modification.

In the second heating scan, the  $T_g$  for the RSCA-treated nanoparticle sample increased at  $25^\circ\text{C}$  and surpassed the  $T_g$  for all nontreated nanoparticle samples. At the same time, the  $T_g$  for the NRSCA-treated nanoparticle sample also increased, reaching the  $T_g$  of the corresponding nontreated nanoparticle sample (3 vol %  $\text{Al}_2\text{O}_3$ ).

We may conclude that in the RSCA-treated nanoparticle sample a stronger filler–matrix interaction exists, due to the chemical reaction between the SCA bonded on the nanoparticle surface (Fig. 2) and the matrix. This strong interaction results in the highest  $T_g$  values among the all composites. The behavior of the NRSCA-treated nanoparticle samples is very close to the behavior of the corresponding nontreated nanoparticle sample (3 vol %  $\text{Al}_2\text{O}_3$ ). This is in the frame of the expected, as NRSCA does not change the filler–matrix interaction.

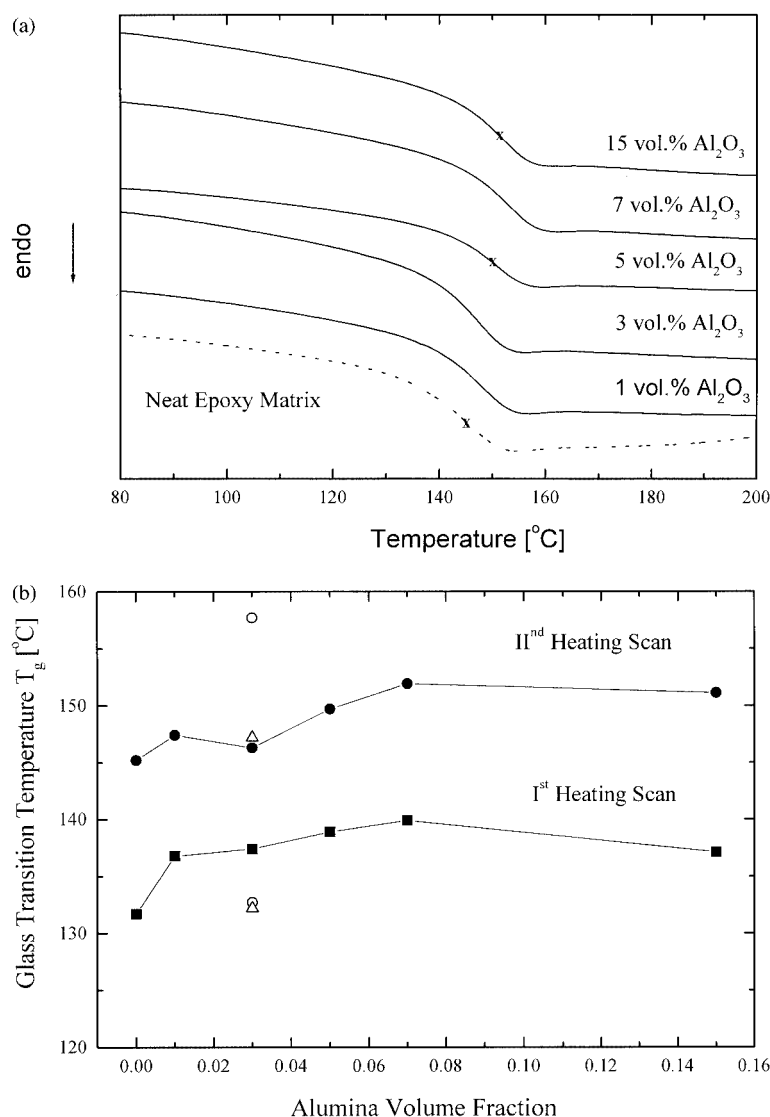


**Figure 1** Results from DSC experiment: (a) second heating DSC scan for neat epoxy matrix and epoxy/nontreated alumina nanoparticle composites with different alumina content ( $T_g$  values are designated with crosses); (b)  $T_g$  as a function of the alumina nanoparticle content: (■) first heating scan and (●) second heating scan for epoxy/nontreated alumina nanoparticle composites; (○) epoxy/RSCA-treated and (△) epoxy/NRSCA-treated alumina nanoparticle composites.

**TABLE II**  
Glass Transition Temperatures,  $T_g$ 's, Detected from DSC Experiment Performed for Epoxy/Alumina Nanoparticle Composites and the Network Density Values, Evaluated by the Storage Modulus Value at the Rubbery Plateau ( $T_g + 50$ )

Sample vol % Al <sub>2</sub> O <sub>3</sub>	$T_g$ (°C) 1 <sup>st</sup> heating	$T_g$ (°C) cooling	$T_g$ (°C) 2 <sup>nd</sup> heating	$M_c$ (g/mol) (from 1 Hz DMTA data)
Neat epoxy resin	131.7	142.2	145.2	1334
1 vol % nontreated	136.8	143.4	147.4	1352
3 vol % nontreated	137.4	143.2	146.3	1360
5 vol % nontreated	138.9	145.5	149.7	1409
7 vol % nontreated	139.9	147.3	151.9	1412
15 vol % nontreated	137.1	148.4	151.1	1413
3 vol % treated with RSCA	132.7	152.8	157.7	1336
3 vol % treated with NRSCA	132.2	134.2	147.2	1489

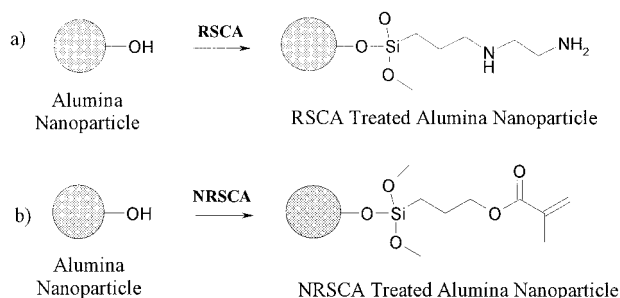


**Figure 2** Scheme of the chemical reactions between the alumina nanoparticle hydroxyl groups and (a) [3-(2-aminopropyl)trimethoxysilane (RSCA) and (b) 3-(trimethoxysilyl)propyl methacrylate (NRSCA).

The network densities, represented by the polymer molecular weight between two points of crosslinking,  $M_c$ , are also presented in Table II. As we mentioned above, these values of  $M_c$  are only for the sake of comparison between the samples investigated in this work. The network density decreases and  $M_c$  increases as the alumina content increases. This fact is often observed for composites. The presence of the filler decreases the local concentration of the crosslinking agent, thus disrupting the crosslinking process and decreasing the network density in the composite compared to the neat matrix.<sup>6</sup>

The RSCA-treated nanoparticle sample has a higher network density, comparable with the network density of the neat epoxy matrix. This is in agreement with the expected chemical reaction between RSCA and the epoxy matrix, which also contributes to the sample network density.

### Results from the DMTA experiment

The activation energies for  $\alpha$  and  $\beta$  relaxations in epoxy/alumina nanoparticle composites were determined by the Arrhenius equation. From their values, using eqs. (2) and (3), we obtained the activation entropy and enthalpy for both relaxations.

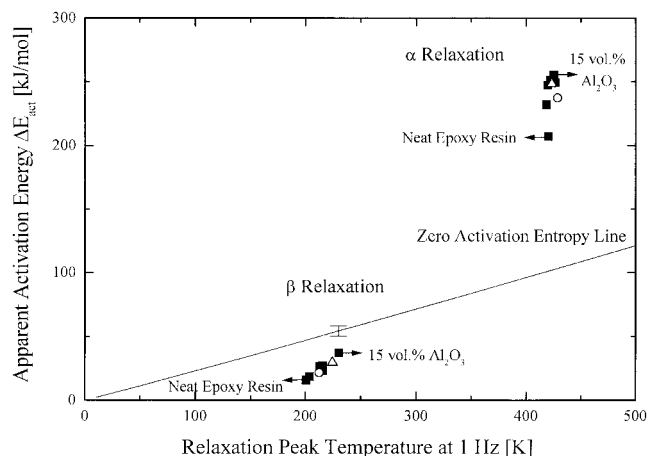


**Figure 3** Epoxy/alumina nanoparticle composites. Dependence of the apparent activation energy on the relaxation peak temperature at 1 Hz for (■) nontreated alumina nanoparticle samples, (○) RSCA-treated alumina nanoparticle sample, and (△) NRSCA-treated alumina nanoparticle sample. The straight line corresponds to zero activation entropy.

### Analysis of the $\beta$ relaxation

The activation energy, enthalpy, and entropy for the  $\beta$  relaxation of the epoxy/alumina nanoparticle composites are shown in Table III together with the  $T_\beta$  values for three frequencies, 1, 10, and 100 Hz. It is obvious that the  $\beta$  relaxation of the epoxy resin is strongly affected by the presence of the alumina nanoparticles. As the alumina content increases to 15 vol %, the activation energy of the  $\beta$  relaxation increases twofold. Naturally,  $T_\beta$  also increases.

The activation energy dependence on the peak temperature at 1 Hz is shown in Figure 3, together with the zero activation entropy line drawn according to eq. (4). The activation energies corresponding to the  $\beta$  relaxations are situated below and not very close to the zero activation entropy line. In fact, the increase of the alumina content shifts the activation energy value closer to the zero activation entropy line (Fig. 3), which means that in the neat epoxy resin, cooperative motions of short scale exist,<sup>1, 2</sup> which are continuously

**TABLE III**  
Activation Energy, Enthalpy, and Entropy and  $T_\beta$  (for 1, 10, and 100 Hz) for the  $\beta$  Relaxation of Epoxy/Alumina Nanoparticle Composites

Sample vol % Al <sub>2</sub> O <sub>3</sub>	$\Delta E_{\text{act}} (\beta)$ (kJ/mol)	$\Delta H^\ddagger (\beta)$ (kJ/mol)	$\Delta S^\ddagger (\beta)$ (J mol <sup>-1</sup> K <sup>-1</sup> )	$T_\beta$ (°C) at 1 Hz	$T_\beta$ (°C) at 10 Hz	$T_\beta$ (°C) at 100 Hz
Neat epoxy resin	16	14	-156	-72.6	-61	-22.9
1 vol % nontreated	18	17	-144	-69.3	-55.1	-25
3 vol % nontreated	27	25	-110	-57.6	-39.9	-24.8
5 vol % nontreated	23	21	-128	-57.5	-31.1	-22
7 vol % nontreated	26	25	-112	-59.9	-40	-28
15 vol % nontreated 3 vol %	37	35	-75	-42.7	-31.1	-16.1
Treated with RSCA 3 vol %	21	20	-134	-60.7	-43.3	-19
Treated with NRSCA	29	28	-104	-48.6	-34.4	-16.1

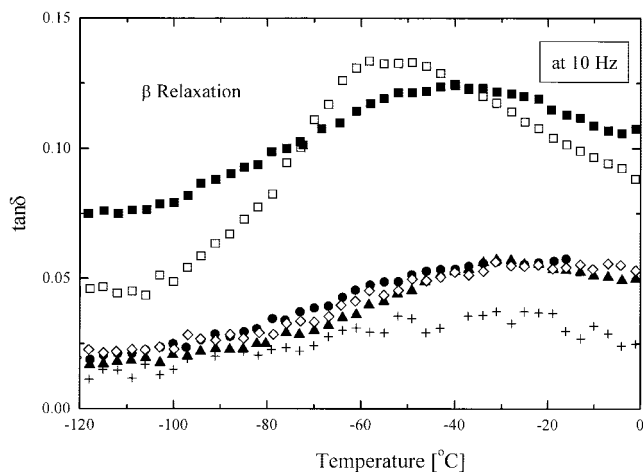


**Figure 4** Temperature dependence of  $\tan \delta$  at 10 Hz for epoxy/nontreated alumina nanoparticle composites with different alumina volume content: (□) neat epoxy resin; (■) 1 vol %; (●) 3 vol %; (▲) 5 vol %; (◇) 7 vol %; (+) 15 vol %.

depressed as the alumina nanoparticle content increases. Respectively, the activation energy values approach the zero activation entropy line.

In Figure 4, the  $\tan \delta$  temperature dependence in the  $\beta$  relaxation region for the neat epoxy resin and all composites containing nontreated alumina nanoparticles are shown. The suppression of the peak intensity is obvious as the alumina content increases. Also, the width of the  $\beta$  relaxation increases, as can be seen in the same figure.

The increase of the activation energy of the  $\beta$  relaxation with the antiplasticizer content is a main characteristic of any antiplasticized system, together with increase of the distribution of the activation energies and, respectively, depression of the  $\beta$  relaxation. We have clearly seen the activation energy increase (Table III) and also the suppression of the  $\beta$  relaxation (Fig. 4) in epoxy/alumina nanoparticle composites as the nanoparticle content increases. We may conclude that the alumina nanoparticles influence the epoxy resin  $\beta$  relaxation in the way a typical antiplasticizer does.

Further, we also used the Starkweather analysis to show the suppression of the short-range cooperative motions related to the  $\beta$  relaxation of epoxy/alumina nanoparticle composites. The values of the activation entropy, according to the Starkweather analysis, could be considered as an indication for the cooperativity of the motions included in the relaxation. The higher the absolute value of  $\Delta S^\ddagger$ , the higher is the cooperative character of the relaxation. The activation entropy of the neat epoxy resin has an absolute value of 156 J/mol K, which corresponds to rather high motional cooperativity. As the alumina content increases,  $\Delta S^\ddagger$  decreases twofold, which means that the nanoparticles hinder the short-scale cooperative motions in the epoxy resin.

It should be noted here that the activation entropies of the neat epoxy resin and all the epoxy/alumina nanoparticle composites are negative. Negative activation entropy means that the activated state has a lower entropy than that of the initial one. A negative value of the activation entropy has already been observed, for example, for the  $\gamma$  relaxation of polystyrene.<sup>11</sup> Its activation entropy is  $\Delta S^\ddagger = -45$  J/mol K, that is, it is smaller than the activation entropies for the  $\beta$  relaxation of the epoxy–alumina nanocomposites observed in this study.

Further proof for the suppression of the short-scale cooperativity in the  $\beta$  relaxation of the epoxy resin could be found in the loss compliance temperature dependence. The result from the subtraction of the neat epoxy resin loss compliance,  $J''_{\text{neat epoxy}}$ , and the loss compliance of the composites containing nontreated alumina nanoparticles,  $J''_{\text{composite}}$ , is presented in Figure 5(a). For the sample with a 1 vol % alumina content, almost no difference compared to the loss

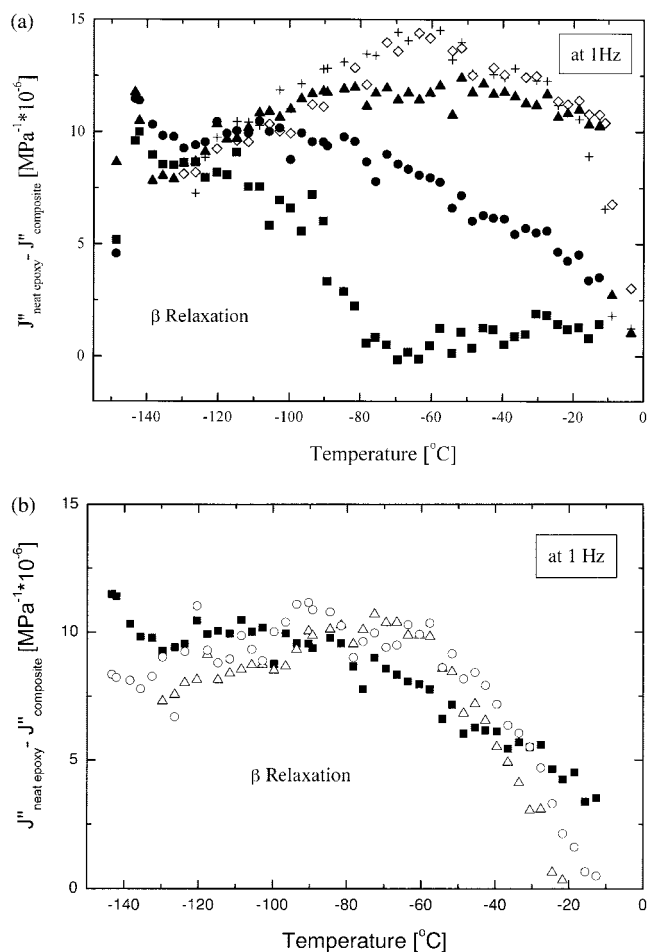


**Figure 5** Temperature dependence of  $J''_{\text{neat epoxy}} - J''_{\text{composite}}$  at 1 Hz: (a) for epoxy/nontreated alumina nanoparticle composites with different alumina volume content: (■) 1 vol %; (●) 3 vol %; (▲) 5 vol %; (◇) 7 vol %; (+) 15 vol %. (b) For 3 vol % alumina: (■) nontreated, (○) RSCA-treated, and (△) NRSCA-treated epoxy/alumina nanoparticle composites.



TABLE IV  
Activation Energy, Enthalpy, and Entropy and  $T_g$  (at 1, 10, and 100 Hz)  
for the  $\alpha$  Relaxation of Epoxy/Alumina Nanoparticle Composites

Sample vol % Al <sub>2</sub> O <sub>3</sub>	$\Delta E_{\text{act}} (\alpha)$ (kJ/mol)	$\Delta H^\ddagger (\alpha)$ (kJ/mol)	$\Delta S^\ddagger (\alpha)$ (J/mol K)	$T_g$ [°C] at 1 Hz	$T_g$ [°C] at 10 Hz	$T_g$ [°C] at 100 Hz
Neat epoxy resin	207	203	252	146.9	157.7	158.8
1 vol % nontreated	232	228	314	145.1	151.9	158
3 vol % nontreated	247	244	349	146.4	149.3	157.7
5 vol % nontreated	251	248	354	149	155.5	161.1
7 vol % nontreated	249	246	344	153.3	155.3	164.3
15 vol % nontreated 3 vol %	255	252	360	151.9	158.1	164
Treated with RSCA 3 vol %	237	234	313	155.3	158.1	167.4
Treated with NRSCA	248	245	346	150.1	152.6	161.3

compliance of the neat epoxy matrix is observed. At further increasing of the alumina content, the higher-temperature part of the difference ( $J''_{\text{neat epoxy}} - J''_{\text{composite}}$ ) increases, which means that the part of the  $\beta$  relaxation due to the short-range cooperative motions decreases as the alumina content increases. At the same time, the low-temperature part, due to the local molecular motions, remains constant. This observation was reported for an antiplasticized epoxy resin.<sup>2</sup> Heux et al.<sup>2</sup> observed the same change of the loss compliance of an epoxy–antiplasticizer system as the antiplasticizer content increases. The similarities observed in the dynamic mechanical spectra of epoxy/alumina nanoparticle composites and antiplasticized epoxy resin originate from the nanolevel dispersed alumina nanoparticles which act as an antiplasticizer for the epoxy resin.

We would like to mention here that there is a difference in the size of one molecule antiplasticizer (which is about 1 nm) and the size of the alumina nanoparticles (which have an average diameter of 40 nm). Just for comparison, the free-volume holes in a polymer glass are estimated to be of the order of 0.5 nm.<sup>12</sup> For the antiplasticizer molecules, it is assumed that they are acting as a constraint for only one repeat unit in the polymer chain (which is of the order of 20 Å), thus disrupting the whole short-scale relaxation process. The nanoparticles that we have used have a size comparable with the length of the smallest segment of the epoxy chain (at least six repeat units), which participate in the short-scale cooperative motions responsible for the higher-temperature part of the  $\beta$  relaxation. Thus, the effect the nanoparticles have is also to disrupt the short-scale cooperative motions as in the case of an antiplasticizer. The difference is that, while the antiplasticizer does it by influencing the motion of one repeat unit, the nanoparticles constrain the motion of the whole segment participating in the short-scale cooperative motion. Thus, the constraint (antiplasticizer molecule or nanoparticle) hinders the short-scale cooperative relaxation motions in

the polymer and has similar effects on the polymer properties.

In Figure 5(b), a comparison between both samples containing SCA-treated nanoparticles and the corresponding sample and nontreated nanoparticles (3 vol % Al<sub>2</sub>O<sub>3</sub>) is presented in terms of the loss compliance difference ( $J''_{\text{neat epoxy}} - J''_{\text{composite}}$ ). The curves for both treated nanoparticle samples are very similar and clearly differ from the curve for the nontreated nanoparticle sample by a further increase in their high-temperature part, which means that the cooperativity in the  $\beta$  relaxation, when the nanoparticles are SCA-treated, is additionally reduced. Probably, the presence of the SCA molecules in these samples also contributes to the antiplasticization.

From the Starkweather analysis and the DMTA spectra of epoxy/alumina nanoparticle composites, we can conclude that adding alumina nanoparticles to the epoxy resin leads to suppression of the  $\beta$  relaxation. This observation could be explained in terms of that the antiplasticization—the alumina nanoparticles act as constraints for the sub- $T_g$  short-scale cooperative motions.

#### Analysis of the $\alpha$ relaxation

The  $\alpha$  relaxation of alumina/epoxy nanoparticle composites is also strongly influenced by the alumina nanoparticles. This can be seen from Table IV, where the activation energy, enthalpy, and entropy and  $T_g$  (at 1, 10, and 100 Hz) for the  $\alpha$  relaxation of the epoxy/alumina nanoparticle composites are presented. The activation energy increases with an increasing alumina content and  $T_g$  also increases.

The  $\alpha$  relaxations usually have high activation energies and activation entropies and are definitely highly complex relaxations. This is clearly seen in Figure 3. Their activation energies are well above the zero activation entropy line, which illustrates their long-range cooperative character. The increase of the activation energy is clearly observed as the alumina content increases (Fig. 3).

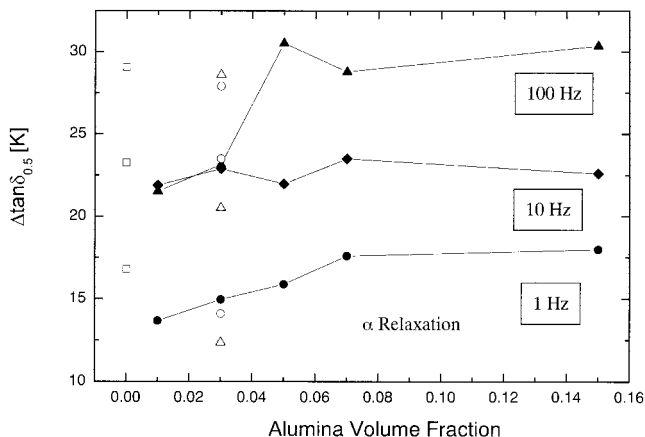


**Figure 6** Half-width of  $\tan \delta$  dependence on the alumina volume content for ( $\square$ ) neat epoxy matrix, ( $\circ$ ) RSCA-treated alumina nanoparticle sample, ( $\triangle$ ) NRSCA-treated alumina nanoparticle sample, and nontreated alumina nanoparticles samples at ( $\bullet$ ) 1 Hz; ( $\blacklozenge$ ) 10 Hz; and ( $\blacktriangle$ ) 100 Hz.

The alumina content dependence of the activation energy obtained by the DMTA experiment coincides with the results obtained from the DSC experiment. The  $T_g$  values obtained from both methods are very close—see the  $T_g$  values obtained in the second heating scan of the DSC experiment (Table II) and the  $T_g$  values obtained from DMTA at 1 Hz (Table IV).

Here, the difference between the present epoxy/alumina nanoparticle system and a common antiplasticized polymer can be seen. The glass transition temperature of an antiplasticized polymer decreases as the diluent content increases, while for our system, the opposite dependence is observed. This difference can be explained by the rigidity of the nanoparticle spheres. If they form clusters, as the lattice model for the antiplasticization suggests, they cannot provide mobility to the polymer chains. Oppositely, they will enhance the restrictions for the segmental mobility of the polymer chains and, hence, the glass transition increases.

The parameters of the  $\alpha$  relaxation for both samples containing SCA-treated nanoparticles are also listed in Table IV. The activation energy and  $T_g$  for NRSCA-treated nanoparticle sample have values close to those of the corresponding sample containing nontreated nanoparticles. In contrast, the RSCA-treated nanoparticle sample has a  $T_g$  that is 10°C higher. The same observation was obtained from the DSC experiment and the explanation given for the DSC results is valid here also.

The half-width of the damping peak as a function of the alumina content is presented in Figure 6. It is clearly seen that the damping half-width increases as the alumina content increases. This fact is typical for the common particulate-filled polymers and it is often taken as an indication for a changed relaxation mech-

anism.<sup>6</sup> Here, also, the broadening in  $\tan \delta$  peak is well defined, but we cannot definitely say that this is a result from a changed relaxation mechanism as this is not always true.

#### Effective thickness of the nanoparticle–matrix interfacial region

From the reduced damping values of  $\tan \delta_c / \tan \delta_m$ , using eqs. (6) and (7), we estimated the thickness of the polymer layer immobilized onto the nanoparticle surface for two temperatures—below and above the  $T_g$ . The calculated values of the layer thickness  $\Delta R$  for all the samples are shown in Table V. For both temperatures,  $\Delta R$  decreases as the alumina content increases. This is explained by the decreasing of the polymer/filler ratio and, hence, the amount of the polymer which is able to wet the nanoparticles. As the alumina content increases to 15 vol %, the weight ratio of the polymer/filler decreases almost 20 times.

For the entire set of samples, the polymer interlayer thickness increases above the  $T_g$  compared to the values below the  $T_g$ . This is probably due to the increased mobility of the polymer chains above the  $T_g$ . For the sample containing 15 vol %  $\text{Al}_2\text{O}_3$ , this increase is insignificant, which proves the explanation for the decreased amount of the polymer, which can wet the nanoparticles. Even though the mobility of the polymer chains is increased, the polymer interlayer adsorbed onto the nanoparticles keeps its thickness constant because the polymer/filler ratio is significantly decreased.

Below the  $T_g$ , the polymer interlayer thickness is larger when nanoparticles are treated with NRSC than when RSCA is used as a treating agent. This is a quite strange result, as we expected stronger interaction and probably a thicker interlayer for the RSCA-treated nanoparticle sample. The properties of these two samples, discussed above, suggest that the filler–matrix interaction in the RSCA-treated nanoparticle sample is stronger. According to the results shown in Table V, the polymer layer adsorbed onto the nanoparticle is thinner at a temperature below the  $T_g$ . Above the  $T_g$ ,

**TABLE V**  
Effective Thickness of the Nanoparticle–Matrix Interfacial Region  $\Delta R$  Below and Above  $T_g$  (from DMTA Data at 10 Hz)

Sample vol % $\text{Al}_2\text{O}_3$	$\Delta R$ (nm)	
	20°C	250°C
3 vol % $\text{Al}_2\text{O}_3$ nontreated	58	81
5 vol % $\text{Al}_2\text{O}_3$ nontreated	50	51
7 vol % $\text{Al}_2\text{O}_3$ nontreated	35	55
15 vol % $\text{Al}_2\text{O}_3$ nontreated	30	32
3 vol % $\text{Al}_2\text{O}_3$ treated with RSCA	41	83
3 vol % $\text{Al}_2\text{O}_3$ treated with NRSCA	65	85

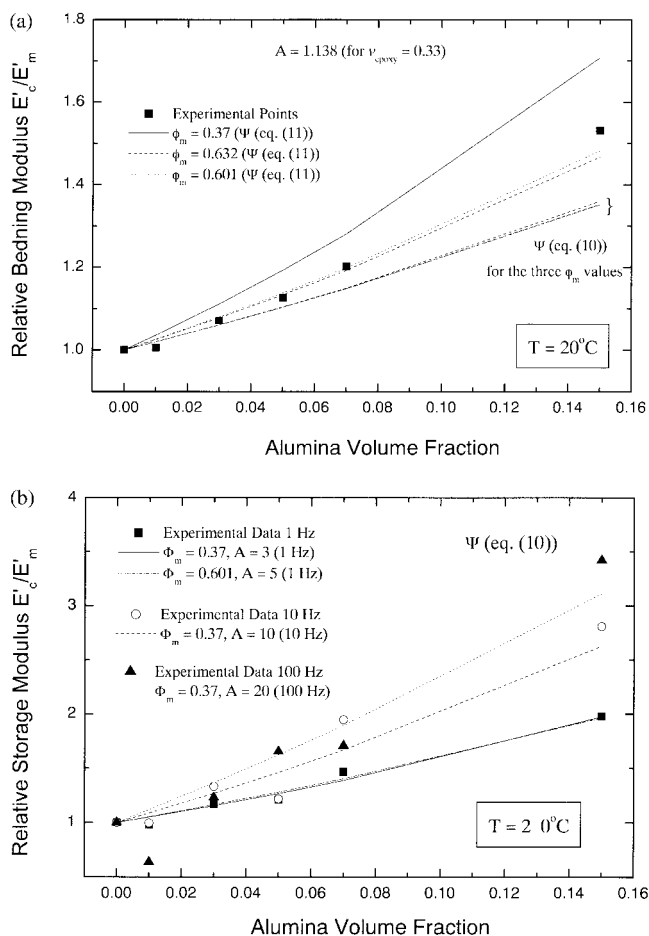


**Figure 7** Relative modulus dependence on the alumina nanoparticle content at (a)  $20^\circ\text{C}$  and (b)  $200^\circ\text{C}$ .

both samples have an almost equal effective thickness of the nanoparticle–matrix interfacial region.

### Reduced modulus dependence on the nanoparticle content

We applied the generalized Kerner equation for the relative modulus of epoxy/nontreated alumina nanoparticle composites. In Figure 7(a), the alumina content dependence of the relative modulus at room temperature (below  $T_g$ ) is presented. The relative modulus values in this figure were obtained by static mechanical measurements in three-point bending mode. These data are presented in more detail in ref. 13. Quite a good fit to 7 vol % alumina is obtained when the generalized Kerner equation is used with the reduced concentration term  $\Psi$  defined by eq. (11). The value of the coefficient  $A = 1.138$  was calculated by eq. (12) for  $\nu_{\text{epoxy}} = 0.33$ . We used three different values for the fitting of the maximum packing fraction:  $\Phi_m = 0.601$  (for random close packing without agglomeration),  $\Phi_m = 0.632$  (for random loose packing without agglomeration), and  $\Phi_m = 0.37$  (for random close packing with agglomeration).<sup>6</sup> The best fit is obtained

when the maximum packing fraction for random close packing without agglomeration of the nanoparticles,  $\Phi_m = 0.601$ , is used. When an agglomeration of the nanoparticles is adopted ( $\Phi_m = 0.37$ ), quite strong deviation of the fitting curve from the experimental data is observed [Fig. 7(a)]. If the reduced concentration term  $\Psi$  is defined by eq. (10), the fitting lines lie below the experimental data no matter what value for  $\Phi_m$  is adopted [Fig. 7(a)].

We can draw the following conclusions for the state of agglomeration in the epoxy/alumina nanoparticle composites at  $20^\circ\text{C}$ , having in mind the best-fitting parameters: The best fit is obtained with  $\Psi$  estimated by eq. (11), which is defined for a system with adopted agglomeration. But the values for both parameters  $\Phi_m$  and  $A$  suggest no agglomeration in the system. So, we can assume the presence of a small number of very strong agglomerates behaving as independent particles at room temperature in the epoxy/alumina nanoparticle composites.

In Figure 7(b), the alumina content dependence of the relative modulus at  $200^\circ\text{C}$  is shown estimated by DMTA curves. A well-defined increase in the relative modulus is observed with an increasing alumina content. The modulus increase above the  $T_g$  is much higher than the one observed at  $20^\circ\text{C}$ , which is consistent with the results for common composites (see Introduction). For the fitting of these results, we used the generalized Kerner equation in which the reduced concentration term  $\Psi$  is defined by eq. (11). The parameter  $A$ , calculated by eq. (12) with Poisson's ratio of  $\nu_{\text{epoxy}} = 0.5$  for rubber, has the value of 1.5. But the best fit at this temperature is obtained when  $A$  has value at least 3, and as the frequency increases, the coefficient  $A$  also increases. Higher values of the constant  $A$  are an indication for the agglomerates' existence. Also, the value of  $\Phi_m$ , corresponding to the agglomeration of the filler particles ( $\Phi_m = 0.37$ ), gives the best fit for the alumina content dependence of the relative modulus at  $200^\circ\text{C}$ . Both parameters,  $A$  and  $\Phi_m$ , have values indicating the presence of agglomerates in the samples at temperatures above the  $T_g$ .

A good explanation for the dependence of the relative modulus of epoxy/alumina nanoparticle composites on the alumina content could be done in terms of particle–particle contacts and agglomeration, which differ below and above the  $T_g$ . At temperatures below the  $T_g$ , a small number of very strong agglomerates exist. Also, below the  $T_g$ , the polymer has a high modulus and can exert large forces on the agglomerates, preventing the motion of the nanoparticles in the agglomerates.<sup>6</sup> Above the  $T_g$ , the polymer matrix is softened; the squeezing forces that the polymer exerts on the agglomerates do not exist any more so particle–particle motion and friction can occur in the agglomerates. In addition, at elevated temperatures, polymer–particle friction or slipping can occur, so at ele-

vated temperatures the agglomerates start to behave as weak ones and that is why the parameters  $A$  and  $\Phi_m$  change their values.

## CONCLUSIONS

### 1. Concerning the $\beta$ relaxation:

- As the alumina content increases, the activation energy and its spread increase, which is a typical characteristic of an antiplasticized system.  $T_\beta$  also increases and the intensity of the  $\beta$  peak decreases.
- The short-range cooperative motions related to the high-temperature part of the  $\beta$  relaxation of the epoxy resin are suppressed as the alumina content increases. This conclusion is proved by the results from the Starkweather analysis and the loss compliance comparison.
- For both SCA-treated nanoparticle samples, the suppression of the high-temperature part of the  $\beta$  relaxation is more pronounced than in the corresponding sample containing nontreated nanoparticles. This is explained by the additional restrictions that SCA molecules insert onto the short-scale relaxation motions.

### 2. Concerning the $\alpha$ relaxation:

- The activation energy of the  $\alpha$  relaxation increases as the alumina content increases, so the glass transition temperature of the epoxy/alumina nanoparticle composites also increases.
  - The glass transition temperature of the RSCA-treated nanoparticle sample is the highest because of the strongest filler–matrix interaction.
3. The effective thickness of the nanoparticle–matrix interfacial region decreases as the alumina content increases, which is explained in terms of a decrease of the polymer/filler ratio.
  4. The relative modulus dependence on the alumina content is very well fitted by the generalized Kerner equation. The three variables—the reduced concentration term  $\Psi$ , the maximum

packing fraction  $\Phi_m$ , and the constant  $A$ —have values suggesting very strong and small agglomerates at room temperature. Above the  $T_g$ , the agglomerates are weak because of the polymer–particle friction or slipping and because of the softening of the polymer matrix.

### 5. The common effects of the rigid fillers on the dynamic mechanical properties of particulate-filled composites are observed for epoxy/alumina nanoparticle composites, namely:

- Increasing of the modulus to a higher extent above the  $T_g$  than below it.
- Broadening of the damping peak accompanied by a slight shift to higher temperatures.

The mechanical properties of the epoxy/alumina nanoparticle composites obtained by static mechanical measurements as well as their wear resistance will be the subject of an article in preparation.<sup>13</sup>

This research was supported through a European Community Marie Curie Individual Fellowship (Contract No. HPMF-CT-2000-00864).

## References

1. Heux, L.; Halary, J. L.; Laupretre, F.; Monnerie, L. *Polymer* 1997, 38, 1767.
2. Heux, L.; Laupretre, F.; Halary, J. L.; Monnerie, L. *Polymer* 1998, 39, 1269.
3. Liu, Y.; Roy, A. K.; Jones, A. A.; Inglefield, P. T.; Ogden P. *Macromolecules* 1990, 23, 968.
4. Ngai, K. L.; Rendell, R. W.; Yee, A. F.; Plazek, D. J. *Macromolecules* 1991, 24, 61.
5. Starkweather, H. W. *Macromolecules* 1981, 14, 1277.
6. Nielsen, L. E.; Landel, R. F. *Mechanical Properties of Polymers and Composites*, 2<sup>nd</sup> ed.; Marcel Dekker: New York, 1994.
7. Nielsen, L. E. *Appl Polym Symp* 1969, 12, 249.
8. Iisaka, K.; Shibayama, K. *J Appl Polym Sci* 1978, 22, 3135.
9. Levita, G.; De Petris, S.; Marchetti, A.; Lazzeri, A. *J Mater Sci* 1991, 26, 2348.
10. Lee, B.-L.; Nielsen, L. E. *J Polym Sci Pol Phys* 1977, 15, 683.
11. Starkweather, H. W. *Macromolecules* 1988, 21, 1798.
12. Anderson, S. L.; Grulke, E. A.; DeLassus, P. T.; Smith, P. B.; Kocher, C. W.; Landes, B. G. *Macromolecules* 1995, 28, 2944.
13. Vassileva, E.; Friedrich, K., in preparation.